CHAPTER IV
RESULTS AND DISCUSSION

4.1 Electrospinning

The fibrous scaffold for tissue engineering is focused on mimicking the extracellular matrix (ECM) because the fibrillar structure of collagen in the ECM plays a crucial role in cell adhesion and growth. Fibrous structure of PHB and PHBV were produced via electrospinning to develop biodegradable scaffolds for tissue engineering. In general, the process of electrospinning is affected by (i) system parameters such as polymer molecular weight, molecular weight distribution and solution properties (e.g. viscosity, surface tension and conductivity), (ii) process parameters such as electrical potential, collective distance and motion of collector, etc. (Z.-M. Huang *et al.*, 2003). Our study demonstrated the feasibility of fiber spinning by varying solution concentration and electrostatic field strength.

4.1.1 Effect of Solution Concentration

Solutions of PHB and PHBV in chloroform were prepared in various concentrations as 10, 12, 14, and 16% w/v. Prior to electrospinning, some properties such as viscosity and conductivity of the as-prepared solutions were measured and the results are summarized in Table 4.1. The viscosity of the resulting solutions were found to increase with increasing solution concentration, while the conductivity was hardly affected by the change in the concentration. The significant increase in the viscosity of the solutions with increasing solution concentration was obviously due to the increased molecular entanglements.

Table 4.1 Solution properties of electrospun fibers

Concentration	Viscosity (cP)		Conductivity 25°C (μs/cm)	
(g/l)	PHB	PHBV	PHB	PHBV
10	366.33	359.33	0.07	0.053
12	633.67	708.33	0.07	0.063
14	1209.00	756.00	0.07	0.07
16	1801.33	1698.33	0.07	0.073

Electrospinning of these solutions was carried out at a fixed applied electrical potential of 12 kV with a fixed collection distance of 20 cm for 5 min. Figures 4.1 and 4.2 show selected SEM images of as-spun fibers from the as-prepared PHB and PHBV solutions having various concentrations. At 10% w/v, non-uniform droplets with slight trace of fibers were obtained (see Figure 4.1a). At such a low concentration, the viscoelastic force (i.e. a result of the low degree of molecular entanglements) in a given jet segment was not large enough to counter the higher Coulombic repulsion force, resulting in the break-up of the charged jet into smaller segments, which, as a result of the surface tension, were later rounded up to form discrete droplets observed. At higher concentrations, the increased viscosity resulted in an increase in the viscoelastic force that was sufficient to prevent the break-up of the charged jet into smaller segments and to allow the Coulombic stress to further elongate the charged jet during its flight to the grounded target which ultimately thinned down the diameter of the charged jet, hence the resulting as-spun fibers. At 12% w/v, a mixture between beaded and smooth fibers was observed (see Figure 4.1b, 4.2b). When the concentration of the solution was increased to 14% w/v, the beads almost disappeared, leaving mostly smooth ultrafine fibers on the target (see Figure 4.1c, 4.2c). In this case, the average fiber diameter was measured to be about 4.3 μm.

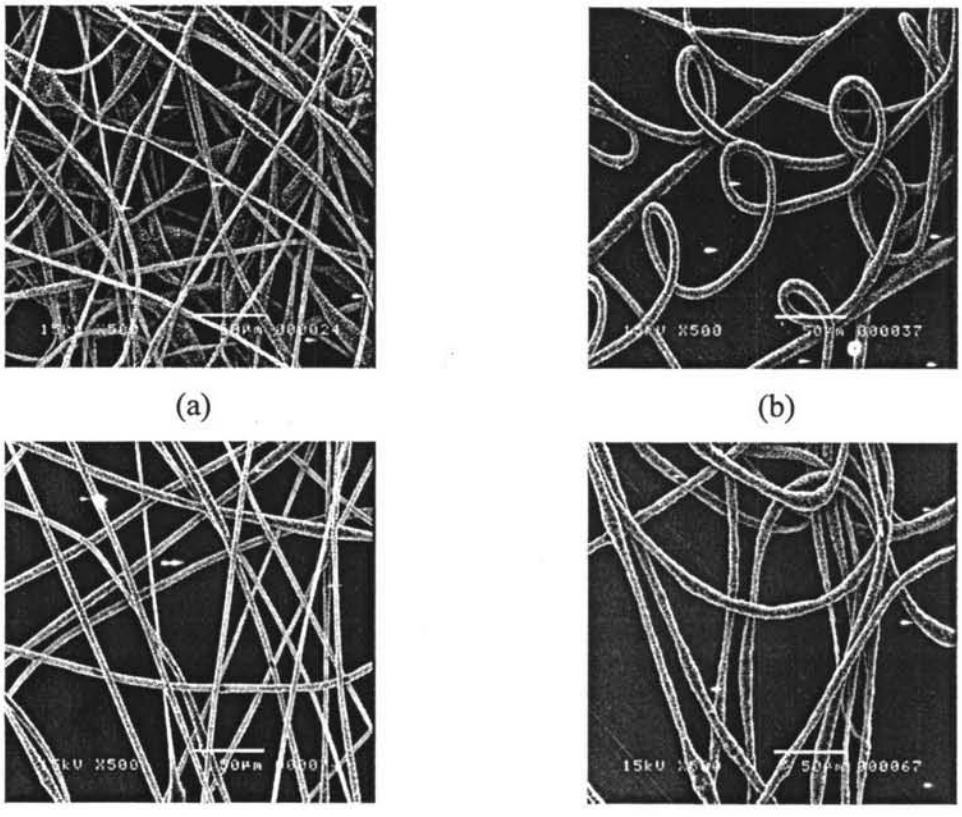

(a) (b)

(c) (d)

Figure 4.1 SEM images (500x) of as-spun fibers from (a) 10, (b) 12, (c) 14 and (d) 16% w/v solutions of PHB in chloroform. The applied electrostatic field strength was 12 kV/ 20 cm and the collection time was 5 min. (scale bar = 50 μm, 500x).

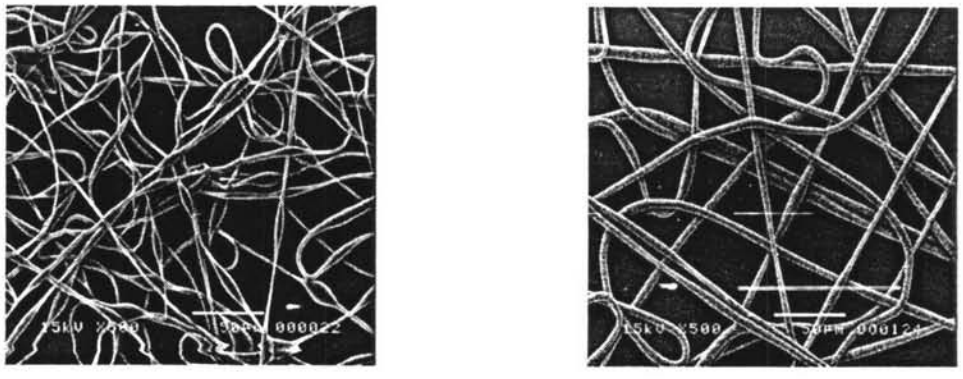

(a) (b)

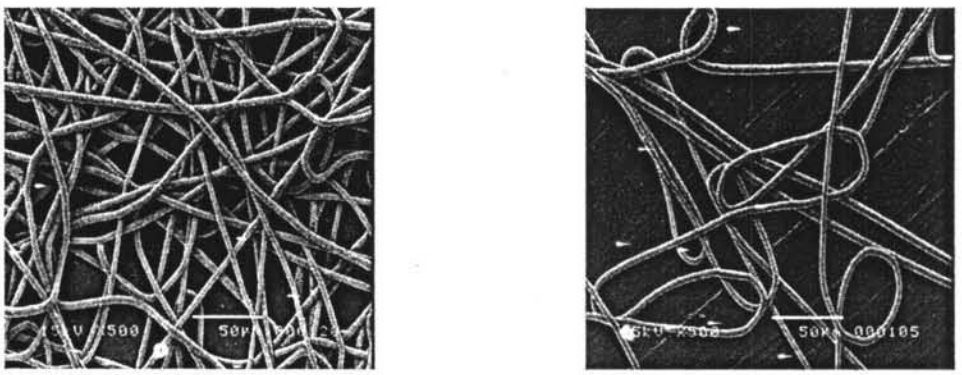

(c) (d)

Figure 4.2 SEM images (500x) of as-spun fibers from (a) 10, (b) 12, (c) 14 and (d) 16% w/v solutions of PHBV in chloroform. The applied electrostatic field strength was 12 kV/20 cm and the collection time was 5 min. (scale bar = 50 μm, 500x).

4.1.2 Effect of Electrostatic Field Strength

To elucidate the effect of the electrostatic field strength on morphological appearance of the as-spun fibers, the electrostatic field strength was varied as 8, 10, 12, and 14 kV over a collection distance of 20 cm for 5 min. Figure 4.3 shows selected SEM images to illustrate the effect of applied electrostatic field strength on morphological appearance of the obtained electrospun fibers from 14% w/v PHB solution under various applied electrostatic potentials, ranging between 8 and 14 kV with a constant tip-to-collector distance of 20 cm. Obviously, beaded fibers were observed at 8 and 10 kV , while mostly smooth fibers were obtained at 12 kV. Figure 4.4 shows selected SEM images of the electrospun fibers from 14% w/v PHBV solution under various applied electrostatic potentials, ranging between 8 and 14 kV/20 cm. Apparently, only smooth fibers without the presence of beads were obtained at all applied electrostatic field strengths investigated.

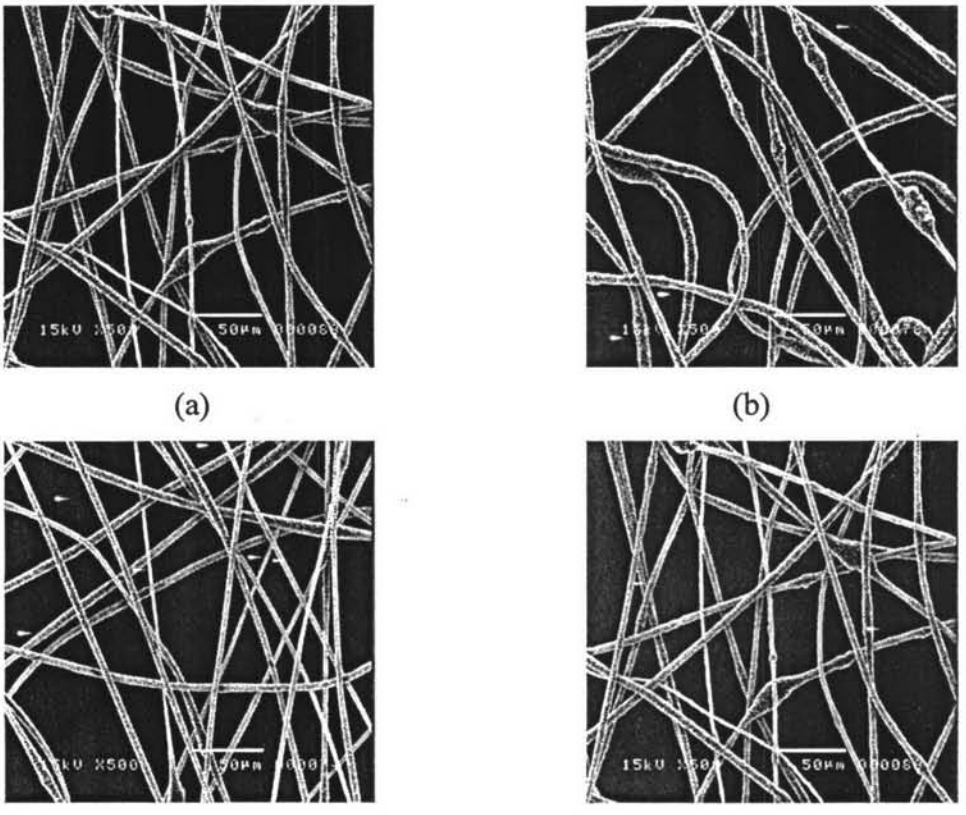

Figure 4.3 SEM images (500x) of as-spun fibers from 14% w/v PHB solutions in chloroform at various applied electrostatic field strengths of (a) 8, (b) 10, (c) 12 and (d) 14 kV/20 cm. The collection time was 5 min. (scale bar = 50 µm, 500x).

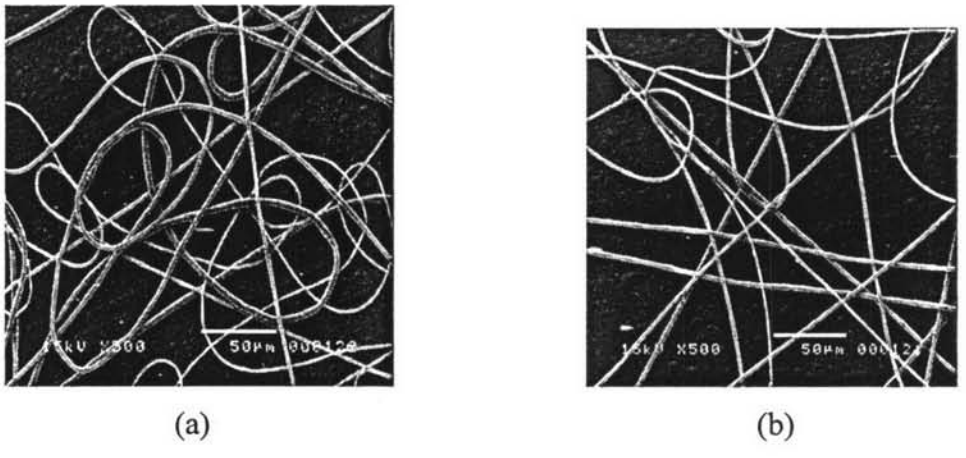

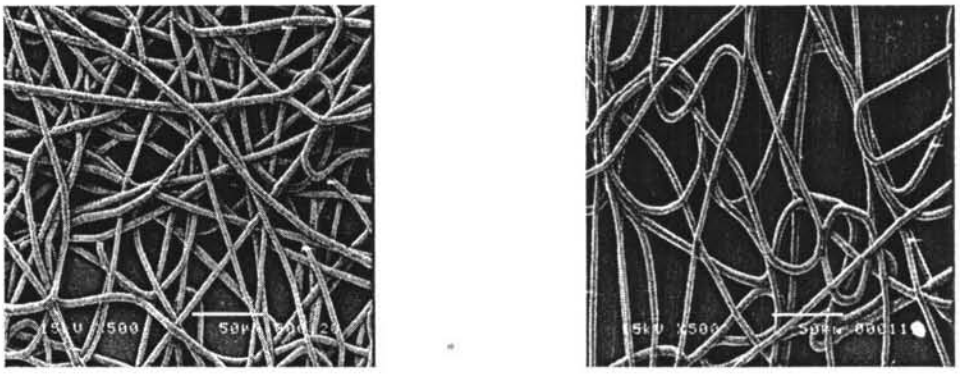

(c) (d)

Figure 4.4 SEM images (500x) of as-spun fibers from 14% w/v PHBV solutions in chloroform at various applied electrostatic field strengths of (a) 8, (b) 10, (c) 12 and (d) 14 kV/20 cm. The collection time was 5 min. (scale bar = 50 μm, 500x).

Clearly, the average diameter of these fibers and fiber density was found to monotonically increase with increasing applied electrostatic field strength (see Table 4.2). Particularly, the average fiber diameter increased from about 2.5 μm at 8 kV/20 cm to about 4.1 μm at 14 kV/20 cm. Since 14% w/v PHBV solution produced very uniform fibers, it was chosen to prepare an as-spun fiber mat for subsequent cell culture studies.

At a higher magnification (5000x), Fig 4.5, it was found that all PHB and PHBV ultrafine fibers had isolated circular shape pores with a narrow size distribution. Interestingly, ultrafine porous fibers were prepared by the rapid phase separation during the electrospinning process when a highly volatile solvent was used. The porous structure was induced by phase separation resulting from the rapid evaporation of chloroform (boiling point = 61.3°C) during the electrospinning process

Table 4.2 Average diameter and bead size of as-spun fibers from 10 and 16% w/v solutions of PHB and PHBV in chloroform with various applied electric field strength

Conc (%w/v)	Electro static field (kV)	Fiber diameter (μm)		Bead size (μm)		Fibers/area (1/100μm^2)		Beads/area (1/100μm^2)	
		PHB	PHBV	PHB	PHBV	PHB	PHBV	PHB	PHBV
10	8	1.6±0.3	1.80±0.5	11.2±4.9	11.9±4.4	12.5±2.5	35.8±5.6	30.5±6.2	24.0±3.1
	10	2.8±0.6	5.54±1.5	7.0+2.2	N/A	65.5±5.3	36.1±4.6	30.1±1.7	N/A
	12	2.9±0.6	1.62±0.4	9.7±3.7	5.5±1.6	65.9±3.6	42.5±6.0	38.7±4.6	25.6±3.3
	14	3.5±0.9	NA	8.1±3.2	N/A	24.3±2.3	N/A	18.5±6.0	N/A
12	8	4.4±1.1	3.18±1.0	51.7±13.5	8.5±3.0	35.6±1.6	25.4±2.9	37.8±4.9	12.2±0.9
	10	1.8±0.5	3.51+1.0	12.0±4.8	N/A	19.7±4.1	58.7+6.6	16.5±6.2	N/A
	12	6.3±1.1	4.66+1.2	N/A	N/A	21.3±6.9	N/A	39.8±3.3	N/A
	14	6.0±2.1	3.80+0.6	17.4±6.6	N/A	61.3±2.6	36.6+2.1	25.7±8.9	N/A
14	8	4.1±1.0	2.54+0.9	8.0±2.8	N/A	35.4±8.7	27.9+0.5	10.7±3.3	N/A
	10	4.4±0.9	2.12±0.67	8.5±2.6	N/A	31.6±3.7	23.7±6.4	9.8±2.2	N/A
	12	4.3+1.0	3.64+0.7	N/A	N/A	40.2+1.6	70.0+4.4	N/A	N/A
	14	3.6±1.0	4.11+0.72	7.7±2.9	N/A	35.7±8.1	29.6+3.4	10.0±3.2	N/A
16	8	8.8±3.2	4.48±0.7	N/A	N/A	70.2±5.5	38.7±8.7	N/A	N/A
	10	5.3±1.3	4.11±0.6	N/A	N/A	42.4±4.7	37.7±4.7	N/A	N/A
	12	6.5±1.6	3.83±0.8	N/A	N/A	41.8±2.2	34.0±2.7	N/A	N/A
	14	N/A	4.04±1.3	N/A	N/A	N/A	48.6±6.2	N/A	N/A

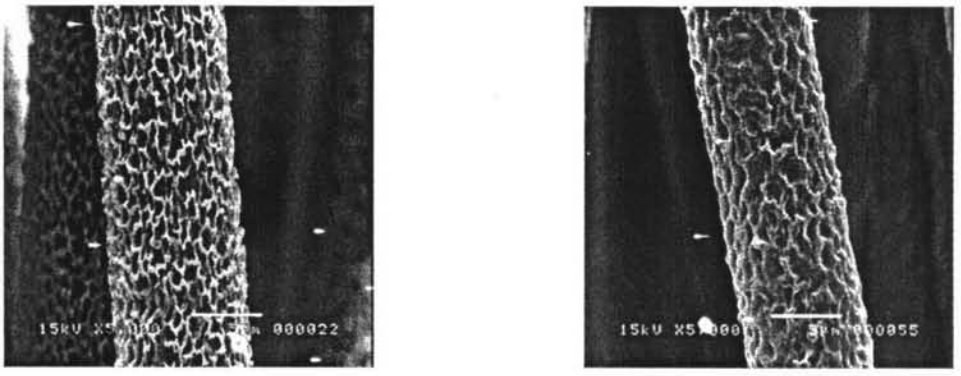

(a) (b)

Figure 4.5 SEM images (5000x) of as-spun fibers from (a) PHB, (b) PHBV at 14% w/v solutions of PHB in chloroform. The applied electrostatic field strength was 12 kV with the collective distance 20 cm (scale bar = 5 μm, 5000x).

4.1.3 Mechanical Properties

The biomaterial should have the appropriate mechanical properties to keep the regenerated tissues in desired sizes and shapes, to provide a temporary mechanical support sufficient to withstand *in vivo* forces exerted by the surrounding tissue and to maintain a potential space for tissue development (Wang *et al.* 2003). PHB and PHBV fibers were electrospun into ~105±5 μm thick fiber mats to measure their mechanical properties. The Mechanical properties, in terms of the tensile strength, Young's modulus, and elongation at break, of the as-spun fiber mats were investigated and the results were illustrated in Table 4.3. The elongation at break of the as-spun PHBV fibers (5.4%) was greater than the as-spun PHB fibers (2.1%), while the tensile strength of the as-spun PHBV fibers (2.0 MPa) was lower than the as-spun PHB fibers (2.5 MPa) because of the content of hydroxyvalerate in PHBV. The homopolymer, PHB, is a relatively stiff, rigid material that has a tensile strength comparable with that of polypropylene. The introduction of a comonomer into this polymer backbone, however, significantly increases the flexibility and toughness of the polymer (extension to break and impact strength), and this is accompanied by a reduction in polymer stiffness (Young's modulus). This is evident in PHBV (Doi, 1990; Sudesh et al., 2000

Table 4.3 Mechanical properties of electrospun fiber mats

	Young's Modulus (MPa)	Tensile strength (MPa)	Elongation at break (%)
PHB	370±275	2.5±0.2	2.1±0.3
PHBV	177±32	2.0±0.2	5.4±3.6

4.1.4 Contact Angle

Wettability was examined by measuring contact angles. At least five reading on different parts of specimens were average for data collecting as show in Appendix D. From Table 4.4, all the contact angle of PHB and PHBV electrospun fiber mats were increased when compare with PHB and PHBV film, meaning that the as-spun fiber mats appeared to be more hydrophobic than the corresponding films.

Table 4.4 Contact angle of distilled water with films and electrospun fibers of PHB and PHBV

PHBV content (wt%)	**Contact angle θ (°)**
Electrospun fibers	
PHB	104
PHBV	102
Casting Films	
PHB	79
PHBV	77

4.2 Cells Growth

Tissue engineering is the use of a scaffolding material to either induce formation of the new cells from the surrounding tissue or to act as a carrier or template for implanting the cells or other agents. The scaffold construct provides the necessary support for cells to proliferate and maintain their differentiated function, and its architecture defines the ultimate shape. The engineering of scaffolds has developed over the years from the initial concept of providing an inert biocompatible construct to allow for revascularization and cell invasion to a tissue engineered approach, whereby the construct is initially seeded with cells, cultured *in vitro*, and finally implanted. It is therefore essential to provide a biological environment in which cells can readily attach, proliferate and maintain their differentiated phenotype and to allow deposition of new bone matrix throughout the entire construct.

4.2.1 Indirect Cytotoxicity

In the structured methodology of biological evaluation of medical devices by in vitro methods proposed by the standard, an essential step is represented by the assessment of test with material extracts on cell cultures (ISO 10993-5). Such a stage avoids direct contact between cells and materials and evaluates the effect of possible toxic contaminants that can be readily extracted from the biomaterial. The cell response when exposed to the extraction media of PHB, PHBV fibrous scaffolds were examined with two cell lines: Schwann cell lines, RT4-D6P2T and mouse fibroblast, L929 cell lines. Fibroblasts were directly in contact in vivo with the implants and are routinely used in laboratory for cytotoxicity test. The MTT assay has been used for in vitro biocompatibility evaluation for its reliability and sensitivity (T. Faber *et al.*, 2001). The rate of extraction vehicles showed no cytotoxic effects on both RT4-D6P2T and L929 cell lines (Fig.4.5) within a given polymer type. Pure 100% v/v vehicle extractions obtained have maintained high cell viability and metabolic activity of RT4-D6P2T and L929. Evidently, for RT4-D6P2T, both PHB and PHBV fibrous scaffold exhibited comparable average absorbance values in compare with control ($p<0.05$; ANOVA). On the other hand, for L929, all given materials exhibited much greater average absorbance values in comparison with that

of the control, with that of the PHBV fibrous scaffold being the greatest, followed by that of PHB fibrous scaffold ($p<0.05$; ANOVA). The obtained results indicated that all given material were not toxic and could be as a good candidate to be used as scaffold.

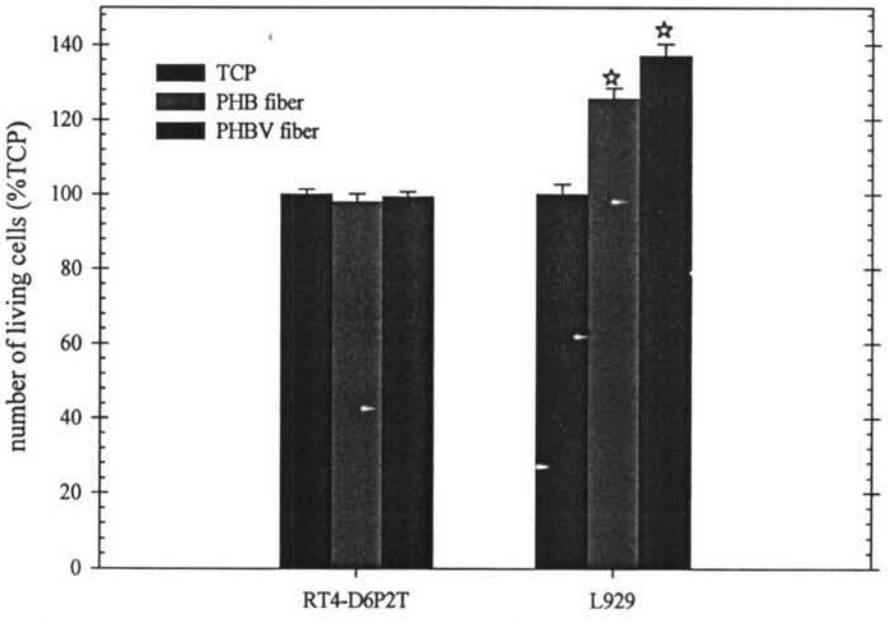

Figure 4.6 The viable metabolic activity of (a) Schwann RT4-D6P2T (b) mouse connective tissue, fibroblast L929 cells cultured for 24 h with PHB and PHBV extracts at 100% concentrations, as determined by MTT assay. * $P<0.05$ vs TCP.

4.2.2 Cell Attachment

In the peripheral nerve degenerating and regenerating process, Schwann cells undergo mitosis and the formation of Schwann cell column is a significant feature between the proximal and distal segments (T.Fabre et al. 2001). After surgical interposition of a bioresorbable implant in the interstump gap, the inner surface of the implant is in direct contact with Schwann cells. Future surgical strategies to restore neurological function in the damaged peripheral nerve tissue may involve replacement of nerve tissue with cultured Schwann cells using biodegrable guide implants (T. Fabre et al. 2001).

Cell morphology on electrospun fibrous and solution-cast film scaffold of PHB and PHBV were usually used to determine the cytocompatibility of a material. The whole process of adhesion and spreading consists of cell attachment, filopodial growth, cytoplasmic webbing, and flattening of the cell mass was in a sequential fashion (Chen, 2004). The effect of the scaffold substrate on Schwann cells culture was observed under the optical microscope and SEM in this study. Observations with the inverted microscope showed that after 24 h incubation (Fig. 4.7), SCs emerged from the explanted nerve tissue fragments and migrated onto the TCP.

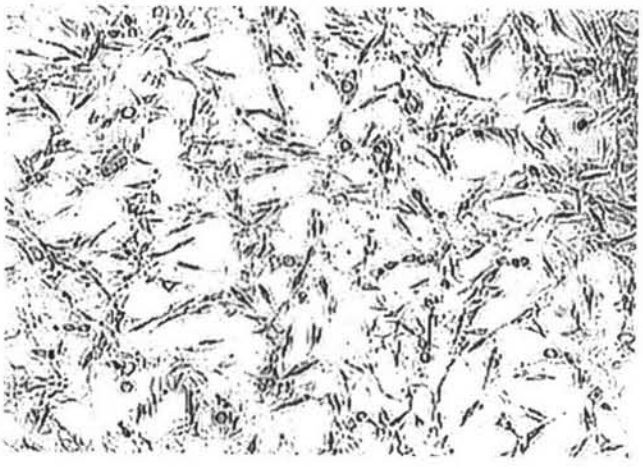

Figure 4.7 Optical microscope (10x) examination of the RT4-D6P2T culture in the culture plate (TCP) after 24h incubation.

The assessment of biocompatibility was conducted by method in which Schwann cells were in direct contact with PHB and PHBV. The present study investigated the effect fibrous and solution-cast film scaffolds of PHB and PHBV on Schwann cell cultures which would occur in vivo during early phase of nerve regeneration through the nerve prosthesis after implantation (T. Fabre *et al.* 2001). The MTT assays have already been used to assess cell proliferation and attachment. This method is rapid, sensitivity and inexpensive method.

PLA have been widely used for over 20 years as surgical sutures, with long established clinical success and many are approved for human use by the FDA

so this study used PLA to be as a control. However, synthetic polymers of the poly(α-hydroxy acids) family release acidic by-products as they undergo degradation by bulk erosion via hydrolysis when exposed to aqueous environments. Although these degradation products are naturally present in the human body and are removed by natural metabolic pathways, the local pH of the surrounding microenvironment can be reduced below that of the natural physiological pH and thus elicit an immunological response. The effect of this acidic environment can cause cell necrosis as well as acting as an autocatalyst, further accelerating the degradation of the polymer.

The time course of Schwann cell MTT reduction activity on scaffolds in each experiment group was showed in Fig.4.8, as determined using MTT assay, which measured mitochondrial dehydrogenase activity of viabie cells spectrophotometrically. MTT assay was employed in this study to quantitatively assess the intensity of color obtained (blue) is directly proportional to the viability and metabolic activity of cell populations and inversely proportional to the toxicity of material. There was not a rapid increasing phase of MTT reduction activity from 2 to 16 h. Initially, there was no significant of SCs viability between PLA and PHBV film but there were greater than PHB both fibrous and corresponding film and PHBV Fibrous scaffold (*$p<0.05$; ANOVA). For longer time, the average absorbance values of Schwann cells attach on all substrates were gradually increased in absorbance value whereas PHBV solution cast film was significant higher than other groups. However, for PHB and PHBV fibrous scaffolds, the MTT reduction activity of Schwann cells indicated a lower level of cell attachment than that on the solution cast film and PLA. The number of cells attached on the different substrates at 16h in culture can be ranked as follows: PHBV film, PLA, PHB film, PHBV fibrous and the PHB fibrous scaffold. The irregularity of the surface morphology might affect the attachment of cells onto the materials. This was the reason why cells attach on solution cast films were faster than on fibrous scaffolds.

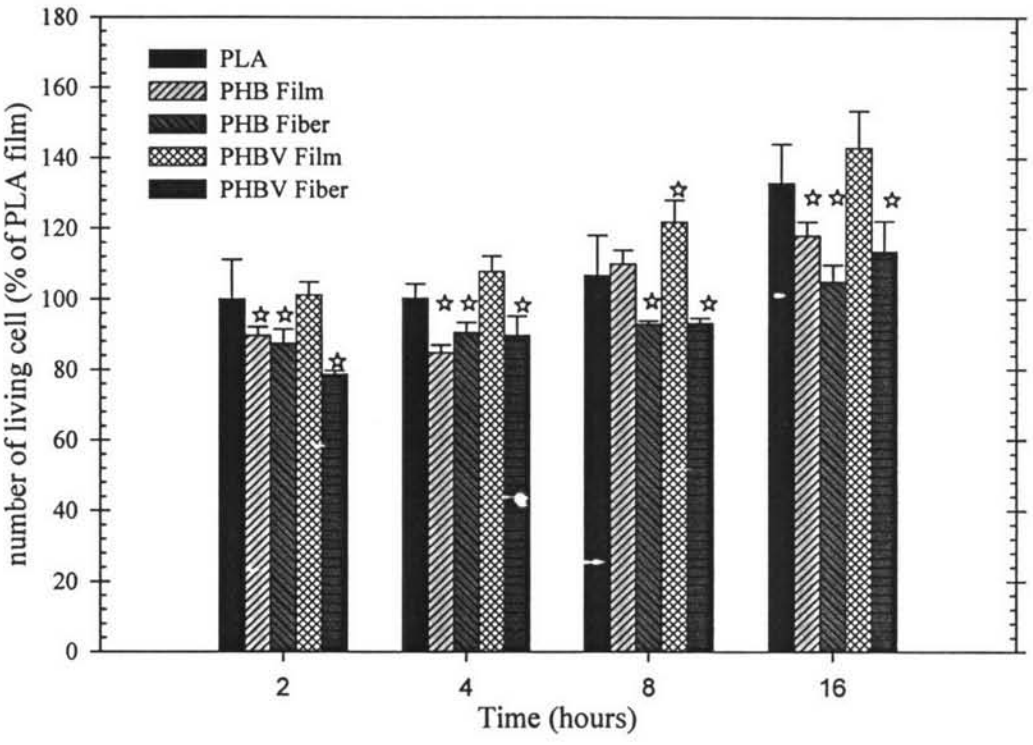

Figure 4.8 The attachment of RT4-D6P2T on PLA (controls), PHB and PHBV films and fibrous scaffolds at 2, 4, 8, and 16h, as determined by the activity of viable cells. .* $P<0.05$ vs PLA.

In order to assess the morphology and cytoplasm architecture of RT4-D6P2T cells on the different substrates, the cells were fixed after 2, 4, 8 and 16h in culture as a monolayer confluence assay. The number of SCs could not be estimated by SEM images due to the fact that the cells were able to penetrate into the inner side of fibrous scaffolds. However, the low-magnification SEM images (Fig. 4.10, scale bar = 50 μm, enlargement 500x) could ensure that there were a plenty of SCs attaching on all types of scaffolds in any culture period. Additionally, the area on the scaffold that the cells occupied also increased with increasing time in culture. Plus, this would be able to support the MTT assay. Fig. 4.11 selected SEM images (Scale bar = 10 μm, enlargement 1500x) showed that, after the cells were seeded for 2h, most Schwann cells attached to the fiber and film surface, showing a spherical shape. After 4h, the cells were stretched out or transformed into a spindle shape and formed cluster. After 8h and 16h, the cells increased in number. The cells covered the fibrous

scaffold and spread their cytoplasm on the fibers. The Schwann cells attached the fiber had round nucleus, abundant cell plasma, well-developed Golgi body and a great quantity mitochondrion (Cheng, 2005), while film scaffolds, SEM revealed that the adherent Schwann cells flattened, the cells took on radiating vortex end to end arrangement. (Fig 4.11).

4.2.3 Cell Proliferation

The effects of different substrates on Schwann cell growth were showed in Fig. 4.9 which demonstrated that the proliferation rate of all substrates was found to increase in absorbance value after day 1 to day 5, demonstrating that the proliferation occurred on all substrates. The proliferation rate at 1 day after seeding, the SCs viability of PHB film was found to be a little lower than other groups while on significant among PLA, PHB fiber, PHBV film and fiber. After 5 days, the viability of SCs on PHB and PHBV fibrous scaffold was found to be lower than that of the film counterpart whereas PHBV film showed the highest absorbance value. The proliferation rate on different substrate can be ranked as follows: PHBV film, PLA film, PHB film, PHBV fibrous and the PHB fibrous scaffold so PHBV can be use as alternative to PLA as a scaffold for nerve regeneration

The proliferation of SCs on PHB and PHBV films was higher than that on PHB and PHBV fibers, while PHBV had more absorbance value than PHB in both film and fibrous scaffold. The reason is that the flat solution cast films may provide more area for settlement of Schwann cells than the as-spun scaffold (Y. Yuan, 2004). Even though the fibrous scaffold served the lower MTT values, they can allow the cells to penetrate inside the scaffold, allow nutrient delivery, metabolic waste removal. [C.T. Buckley, 2004].

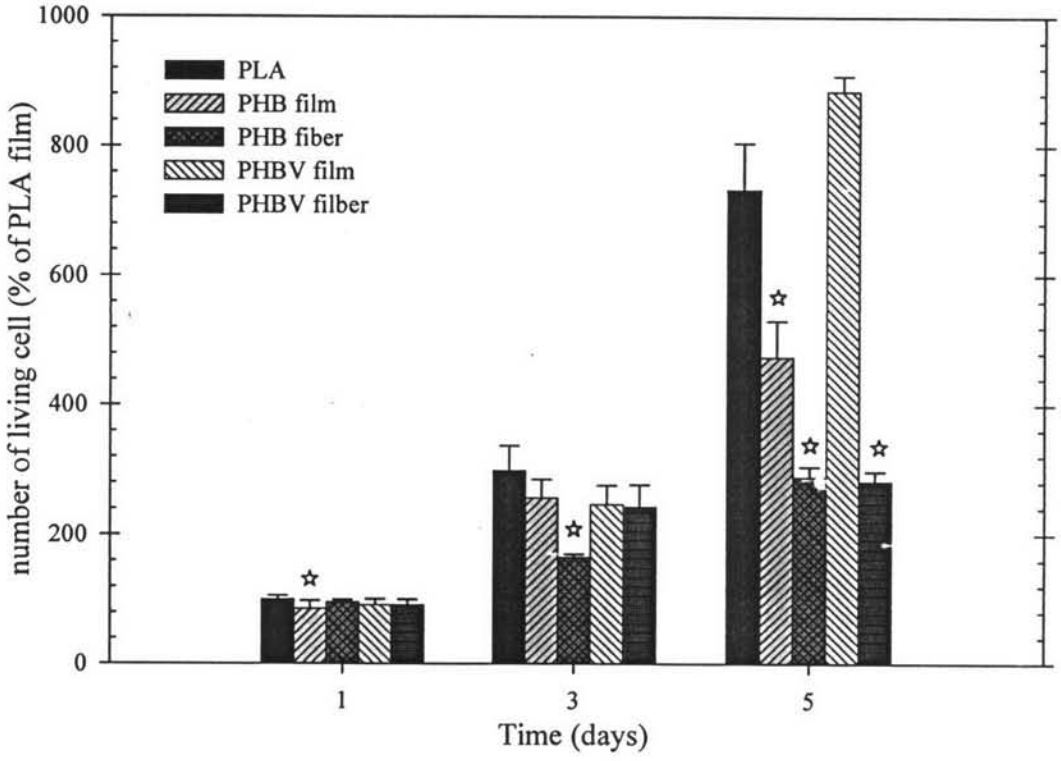

Figure 4.9 The proliferation of RT4-D6P2T on PHB and PHBV fibrous scaffolds, film and PLA (controls) at 1, 3 and5 days, as determined by the activity of viable cells.

SEM examination also revealed that the Schwann cells flattened and extended in a sequential fashion after being cultured for 1, 3, and 5 d on solution cast film whereas SCs appeared to stretch out and demonstrate a typical bi- or tripolar morphology with oval nuclei on fibrous scaffold (fig. 4.12). This cell morphology corresponded to a previous work in which Schwann cells were cultured onto a flat surface like film [Chatelet C. et al., 2000]. In a more recent report [Yuan Y. et al., 2003], after 1 day in culture, the split of SCs indicated that proliferation occurred. After 5 d in culture, we observed that, in comparison with the adherence of SCs onto PHA fibrous scaffold, that on PHA solution-cast film were more densely distributed. A large number of cells migrated into the material and the cell layers reached confluence. The increase in number of cells on the solution-cast films and PLA (control), as observed in SEM images, revealed that the adherent Schwann cells

flattened, connected to each other and extended over film scaffold and glass surfaces. The adherent Schwann cells connect to each other and extended along the PHB and PHBV fibrous scaffold. SCs were observed to grow in multilayer fashion on PHB and PHBV fiber and grew between neighboring fibers. The bipolar cells could encircle the fibers. This is clearly illustrated by comparing the cells after 3 and 5 d in culture (Fig. 4.12, enlargement 500x and Fig. 4.13, enlargement 1500x) to the cells after 1 d in culture.

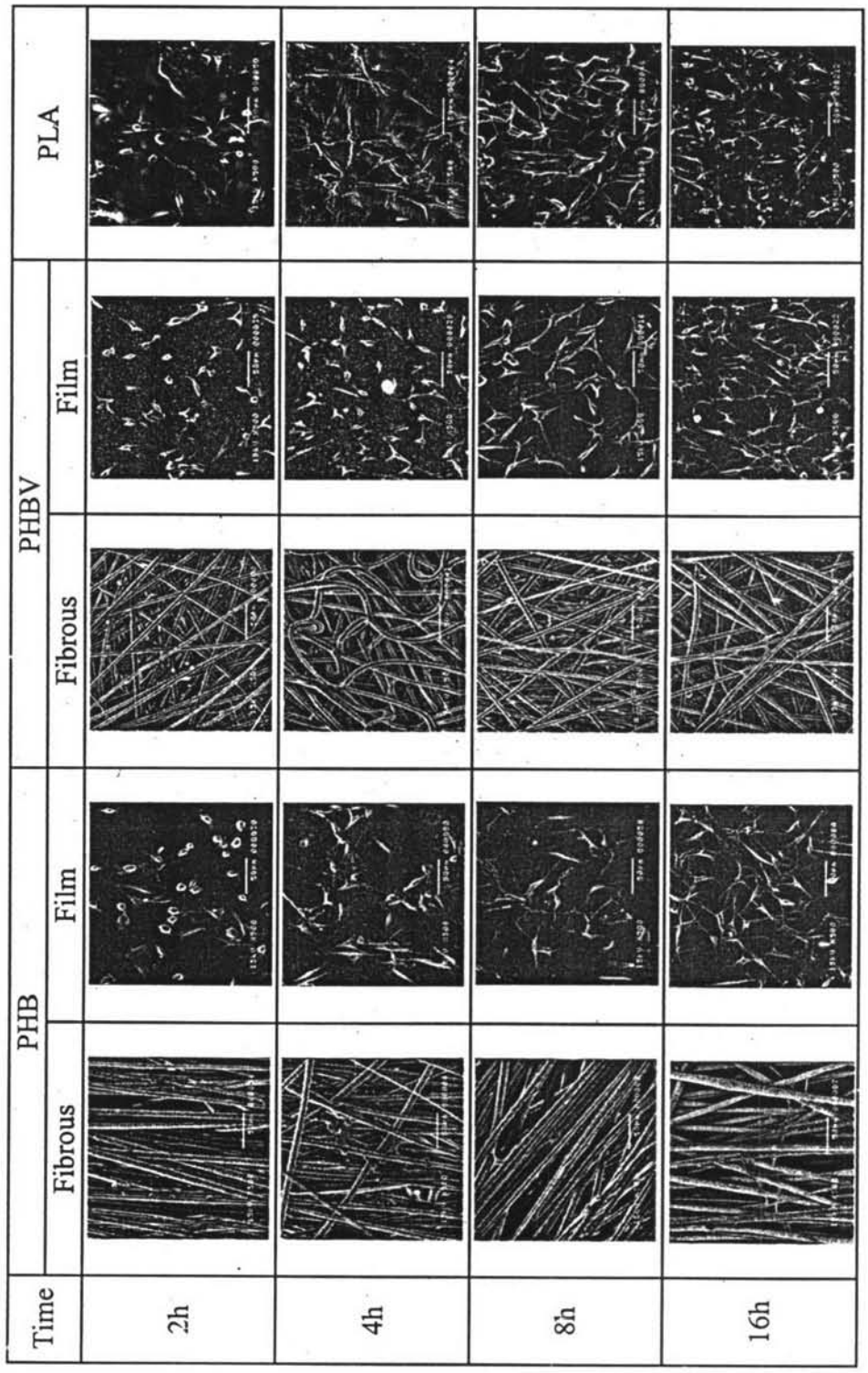

Figure 4.10 The Morphological appearance of SCs cultured on PHB and PHBV fibrous scaffolds, film and PLA (control) at 2, 4, 8 and 16h after seeding. (Scale bar = 50 μm, 500x).

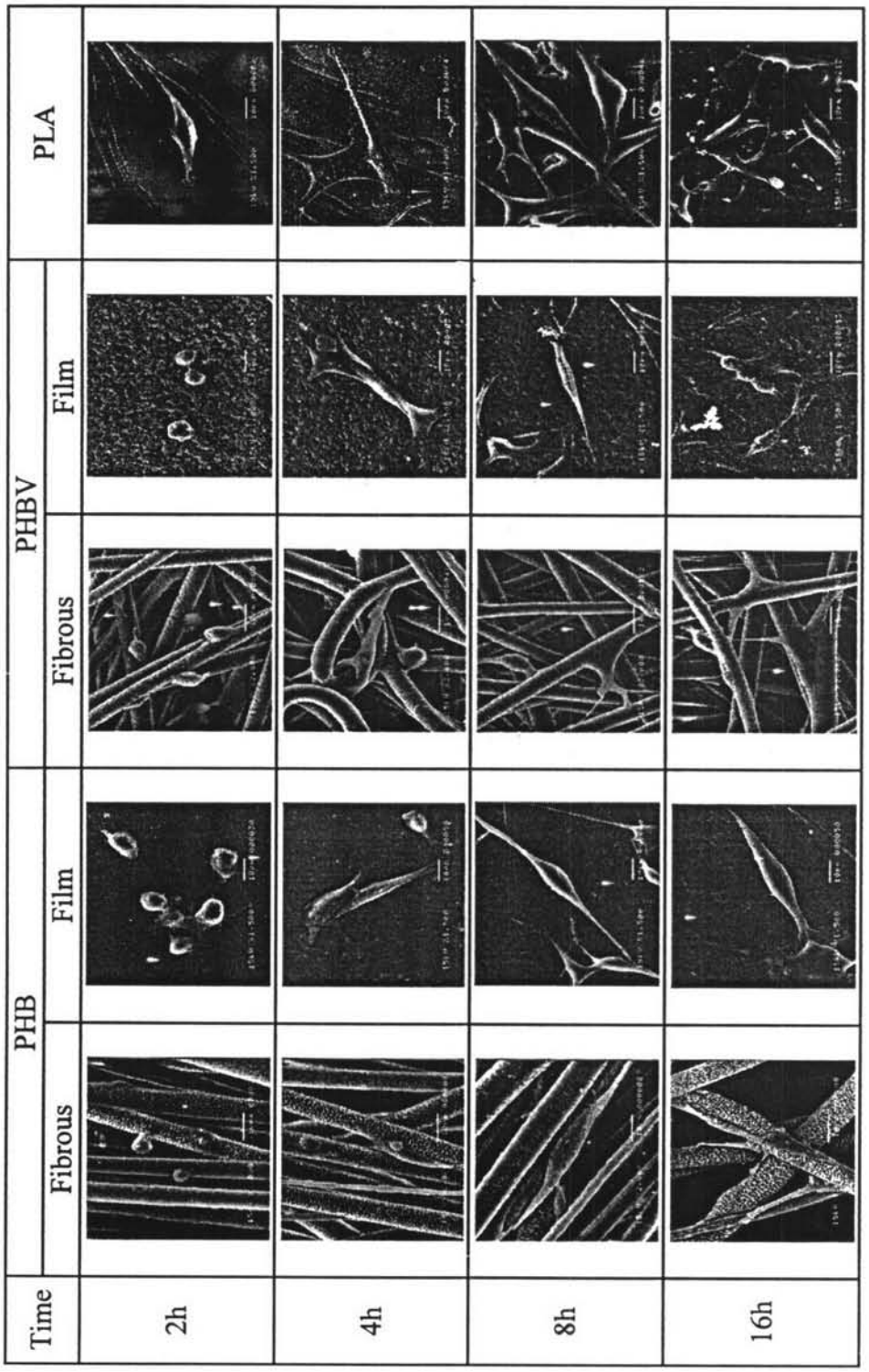

Figure 4.11 The Morphological appearance of SCs cultured on PHB and PHBV fibrous scaffolds, film and PLA (control) at 2, 4, 8 and 16h after seeding. (Scale bar = 10 μm, 1500x).

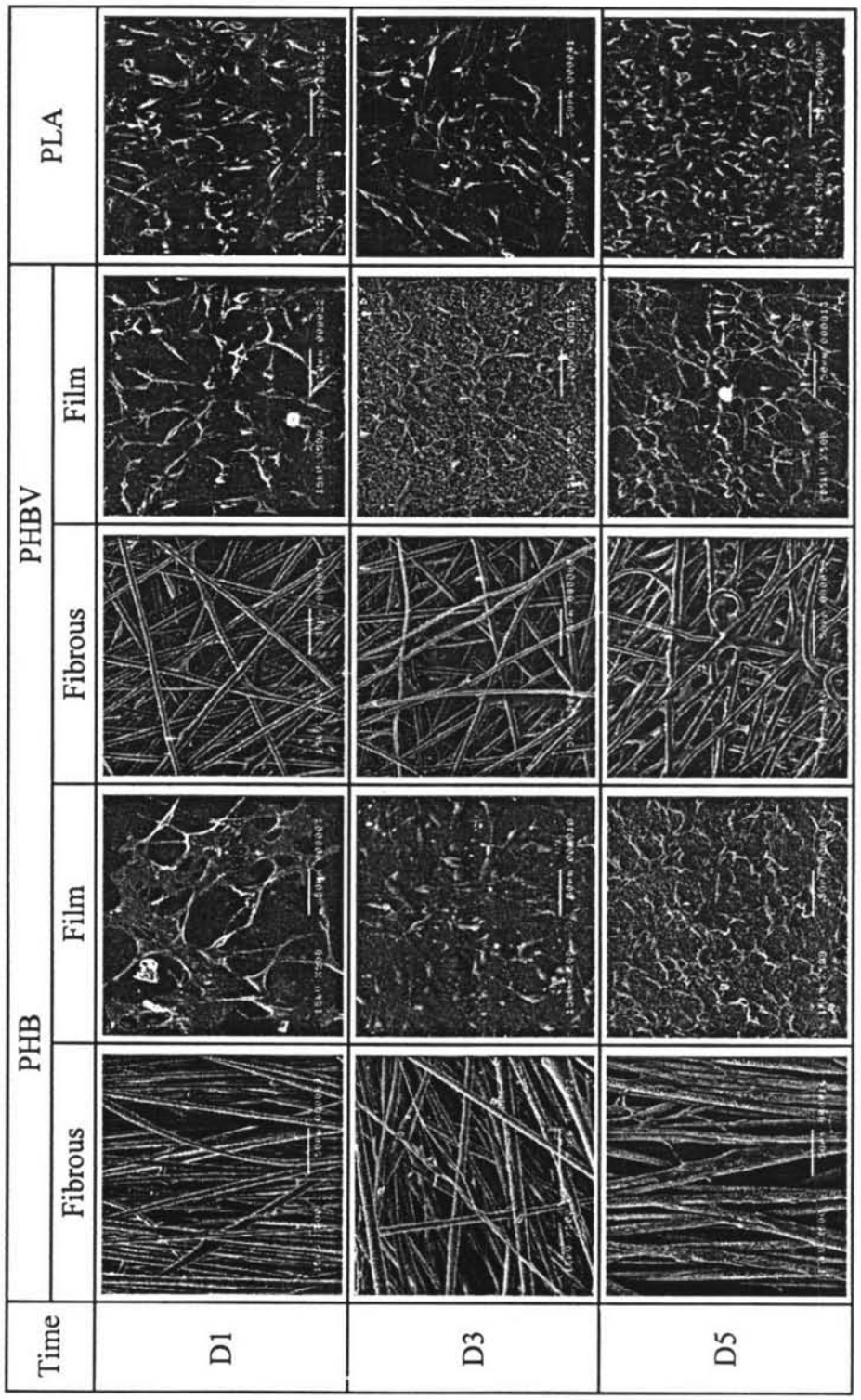

Figure 4.12 The Morphological appearance of SCs cultured on PHB and PHBV fibrous scaffolds, film and PLA (control) at 1, 3 and 5 days after seeding. (Scale bar = 50 μm, 500x).

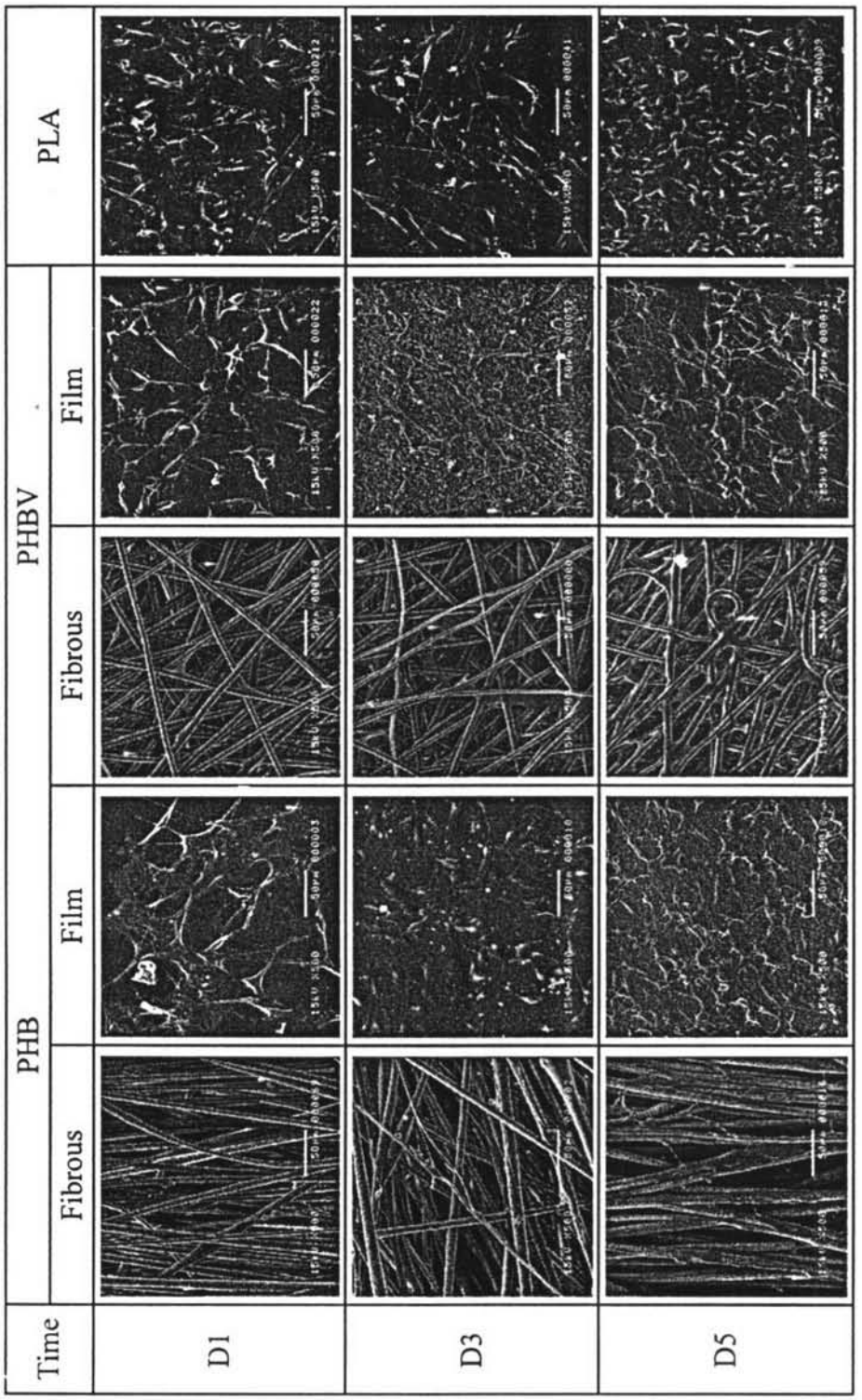

Figure 4.13 The Morphological appearance of SCs cultured on PHB and PHBV fibrous scaffolds, film and PLA (control) at 1, 3 and 5 days after seeding. (Scale bar = 10 μm, 1500x).